A Novel Multiepitope Vaccine for Jembrana Disease: Immunoinformatics, Structural Analysis, Molecular Docking, and Molecular Dynamics

Fatimah Fatimah[1,2], Syahputra Wibowo[3], Dini Wahyu Kartika Sari[1,4], Rarastoeti Pratiwi[1,5], and Asmarani Kusumawati[1,6*]

[1]*Study Program of Doctor in Biotechnology, Graduate School, University of Gadjah Mada, Teknika Utara, Yogyakarta 55281, Indonesia*

[2]*Department of Medical Laboratory Technology, STIKES Karya Putra Bangsa, Jl. Raya Tulungagung - Blitar Km. 4, Tulungagung 66291, Indonesia*

[3]*Eijkman Research Center for Molecular Biology, National Research and Innovation Agency, Meatpro Building, Soekarno Science and Technology Area (KST), Jl. Raya Jakarta-Bogor Km. 46 Cibinong, Bogor 16911, Indonesia*

[4]*Department of Fisheries, Faculty of Agriculture, Universitas Gadjah Mada, Jl. Flora, Yogyakarta 55821, Indonesia*

[5]*Faculty of Biology, Universitas Gadjah Mada, Jl. Teknika Selatan, Sekip Utara, Yogyakarta 55281, Indonesia*

[6]*Department of Reproduction and Obstetrics, Faculty of Veterinary Medicine, Universitas Gadjah Mada, Jl. Fauna No. 2, Karangmalang, Yogyakarta, 55281, Indonesia*

* ***Corresponding author:***

email: uma_vet@ugm.ac.id

Received: August 28, 2025
Accepted: October 7, 2025

DOI: 10.22146/ijc.110759

Abstract: *Jembrana disease, caused by the Jembrana virus, leads to high mortality (30%) and abortion (49%) in cattle, making vaccination essential. In this study, a multiepitope vaccine was designed using immunogenic TM and CA proteins. Predicted cytotoxic T lymphocyte, helper T lymphocyte, and linear B-cell epitopes were linked with flexible linkers, and the 50S L7/L12 ribosomal protein was added as a TLR4 agonist.* In silico *analysis confirmed the construct as non-allergenic, antigenic, and thermostable (aliphatic index 85.44), with 94.2% of residues in favored Ramachandran regions. Docking analysis revealed strong binding to TLR4 (−66 kcal/mol), and molecular dynamics simulations validated the structural stability. Immune simulations revealed increased antigen and antibody levels (IgM early, IgG1/IgG2 after day 15), progressive CD4+ T-helper expansion, transient CD8+ T-cell peaks, elevated IFN-γ and IL-2, and strong dendritic cell activation through MHC I and II pathways. These findings indicate the vaccine effectively stimulates humoral and cellular responses, supporting its potential as a promising candidate against the Jembrana virus.*

Keywords: *immunoinformatics;* in silico *cloning; Jembrana disease virus; molecular docking; multiepitope vaccine*

■ INTRODUCTION

Jembrana disease, caused by the Jembrana virus, affects Bali cattle and their offspring with mortality up to 30% and abortion up to 49% during the acute phase [1]. These high rates result in substantial economic losses and hinder national beef production. Initially restricted to Bali, the disease has spread to West Sumatra, Lampung, East Java, and Kalimantan [2]. Vaccination remains a key strategy for controlling and preventing the spread of viral diseases. For Jembrana disease, the available vaccine is an inactivated vaccine derived from the spleens of infected cattle, treated with Triton X-100 [3]. While this vaccine can reduce clinical symptoms, its effects on the cellular immune response and long-term viral persistence remain unclear [4]. Post-vaccination challenge studies have also shown that immunized cattle may still test positive for Jembrana virus infection [3].

Recombinant strategies have recently been explored. A DNA vaccine delivered via PLGA nanoparticles has reached the *in vitro* evaluation stage [5]. However, DNA vaccines still raise safety concerns, including autoimmune risks, genome integration, and possible mutagenesis [6]. These limitations highlight the need for safer and more effective alternatives.

Multiepitope vaccines offer a promising solution. Composed of sequential or overlapping peptides, they are designed to elicit targeted immune responses and block viral infections [7]. The selected peptides are derived from viral structural and non-structural proteins that play essential roles in entry and replication within host cells [8]. Compared to whole-protein, live-attenuated, or inactivated vaccines, peptide-based multiepitope vaccines enable the precise selection of antigens, thereby avoiding non-beneficial epitopes that may weaken immune responses [9].

This approach has also been applied successfully to livestock diseases. For example, multiepitope constructs have been designed against *Anaplasma marginale* [10], Lumpy Skin Disease virus [11], *Brucella* spp. [12], and Bovine Viral Diarrhea virus [13]. These studies confirmed construct stability through molecular docking and dynamics and predicted robust humoral and cellular responses in *in silico* immune simulations. Such findings reinforce the relevance of this strategy for developing safe and effective vaccines in cattle. Computational vaccinology further accelerates vaccine development by enabling rapid prediction of immunogenic targets while reducing costs and animal use [14]. Comparable strategies have been applied in drug discovery, including network pharmacology and docking for anticancer compounds [15], QSAR and dynamics for antimalarial inhibitors [16], and computational screening of HER2 inhibitors [17]. Immunoinformatics also permits simulation of T- and B-cell recognition, MHC coverage, cytokine release, and antibody kinetics, providing early insights into vaccine efficacy. Here, a multiepitope vaccine against Jembrana virus was designed using reverse vaccinology. Epitopes from TM, involved in viral–host fusion [14], and CA, a dominant antibody target [4], were linked with peptide spacers and fused to the 50S ribosomal protein L7/L12 as a TLR4 agonist. The construct was evaluated through antigenicity, allergenicity, toxicity, and structural analyses, followed by molecular docking, dynamics, immune simulation, and *in silico* cloning to assess potential immunogenicity and expression.

■ EXPERIMENTAL SECTION

Materials

The materials used in this study for the design of the multiepitope vaccine construct included the transmembrane (TM) and capsid (CA) protein sequences of the Jembrana disease virus strain Tabanan 1987, as well as the ribosomal protein L7/L12 sequence. The ribosomal protein sequence was retrieved from UniProtKB with accession number P9WHE3.1, while the Toll-like receptor 4 (TLR4) receptor sequence of *Bos indicus* was obtained from the GenBank database with accession number KX138607.1.

Additionally, various online and standalone software tools were utilized throughout the study. The online tools included the IEDB Analysis Resource, IEDB TepiTool, NetBoLAIIpan 1.0 server, SOPMA, AlphaFold 2, GalaxyRefine, ERRAT, PDBsum Generate, ProtParam, VaxiJen v2.0, AllerTOP v2.0, ToxIBTL, SwissModel, GRAMM Docking, PRANKWEB, CABS-Flex 2.0, Java Codon Adaptation Tool (JCat), the Takara Cut-Site Navigator, and C-IMMSIM. The standalone software used consisted of PyMol molecular graphics system, Discovery Studio Visualizer 2016, and SnapGene software.

Instrumentation

All computational analyses were performed using a Lenovo Ideapad Slim 3i laptop equipped with an Intel Core i7 processor and running Windows 11 Home Single Language.

Procedure

Data mining of immunogenic protein sequences and the TLR4 receptor

In this study, the immunogenic protein sequences of the TM and CA proteins of the Jembrana virus Tabanan 1987 strain were obtained from previously published research data [7,18]. The complete sequence of the Bos indicus TLR4 was retrieved from the GenBank

database under accession number KX138607.1. The TLR4 receptor, a protein located on the surface of various cell types [19], was selected as the target receptor for interaction with the multiepitope vaccine, as the specific host receptor for the Jembrana virus has not yet been identified.

Epitope analysis of the TM and CA proteins of the Jembrana virus Tabanan 1987 strain

B-cell epitope prediction of the immunogenic TM and CA proteins was performed *in silico* using the IEDB Analysis Resource (http://tools.iedb.org/main/bcell/). Three prediction methods were utilized, including BepiPred Linear Epitope Prediction 2.0, Emini Surface Accessibility Prediction, and Kolaskar & Tongaonkar Antigenicity. Cytotoxic T lymphocyte (CTL) epitope prediction was conducted using the IEDB TepiTool (http://tools.iedb.org/tepitool/) with the *Bos taurus* MHC class I allele parameter (BoLA-D18.4) [14]. Helper T lymphocyte (HTL) epitope prediction for MHC class II was carried out using the NetBoLAIIpan 1.0 server (https://services.healthtech.dtu.dk/services/NetBoLAIIpan-1.0/) with the *Bos taurus* DRB3 allele as a parameter [20]. These analyses enabled the identification of short peptide epitopes from TM and CA proteins that are potentially recognized by B cells and T cells.

Multiepitope vaccine construct design

During the design of the multiepitope vaccine construction, the vaccine components are arranged consecutively according to the research on multiepitope vaccine development for SARS-CoV-2 conducted by Yu et al. [21], which begins with an adjuvant in the N-terminal part. In this study, we utilized 50S ribosomal L7/L12, a TLR4 agonist. In the following, we added EAAAK (Glu-Ala-Ala-Ala-Lys) rigid linker, CTL (Cytotoxic T Lymphocyte) epitope, HTL (Helper T Lymphocyte) epitope, and LBL (Linear B Lymphocyte). In this study, a TLR4 agonist, ribosomal 50S L7/L12, was added to the N-terminal part of the vaccine construction to serve as an adjuvant [12]. In the construction of multipitope vaccines, the CTL peptide is linked to the AAY (Ala-Ala-Tyr) linker, the HTL peptide is linked to the GPGPG (Gly-Pro-Gly-Pro-Gly) linker, and the LBL peptide is linked to the KK (Lys-Lys) linker. The construction scheme of the Jembrana disease multiepitope vaccine is shown in Fig. 1.

3D structure prediction, structure optimization, and quality validation of a multiepitope vaccine

The multiepitope vaccine was then subjected to secondary structure analysis to determine the composition of α-helix, β-sheet, and coil in the construct using the online program SOPMA (https://npsaprabi.ibcp.fr/cgibin/npsa_automat.pl?page=/NPSA/npsa_sopma.html) [22]. Then, it was modeled in 3D by submitting the construct sequences into the AlphaFold 2 online program (https://colab.research.google.com/github/sokrypton/ColabFold/blob/main/AlphaFold2.ipynb) [23]. Once modeled, the structure was optimized using GalaxyRefine Server (https://galaxy.seoklab.org/) [24]. The refined vaccine structure was verified using ERRAT (https://saves.mbi.ucla.edu/). Structure verification using ERRAT was performed based on crystallography [25]. The quality of multiepitope vaccine construction was validated by analyzing Ramachandran plots obtained from PDBsumGenerate (https://www.ebi.ac.uk/thorntonsrv/databases/pdbsum/Generate.html) [26].

Physiochemical analysis, antigenicity, allergenicity, and toxicity of multiepitope vaccine constructs

Multiepitope vaccine constructs were analyzed for their physicochemical properties, including molecular weight, amino acid composition, instability index, half-life, and pI, using the ProtParam online program (https://web.expasy.org/protparam/) [27]. The antigenicity, allergenicity, and toxicity of the multiepitope vaccine construct were evaluated to ensure its safety profile [28]. Multiepitope vaccine constructs must weigh less than 110 kDa to facilitate purification [21]. Multiepitope vaccine constructs were predicted for antigenicity using the online program VaXijen v2.0 (http://www.ddg-pharmfac.net/vaxijen/scripts/VaxiJen_scripts/VaxiJen3.pl) with a threshold of 0.4 [29]. A vaccine is considered antigenic if it has an antigenicity value of more than 0.4. Vaccine construction was also predicted for its allergenicity using the AllerTOP v2.0 online program (https://www.ddgpharmfac.net/AllerTOP/feedback.py) [30], and its toxicity using the ToxIBTL program (https://server.weigroup.net/ToxIBTL/

Server.html) [31].

Molecular docking between the vaccine and TLR4

Molecular docking was performed to determine the interaction ability between the vaccine and TLR4, a universal receptor. The TLR4 structure was obtained from modeling the TLR4 sequence of *Bos indicus* using the SwissModel online program (https://swissmodel.expasy.org/interactive) [32]. The quality of the TLR4 receptor model structure was determined from the Ramachandran plot that was obtained from PDBsum Generate (http://www.ebi.ac.uk/thorntonsrv/databases/pdbsum/Generate.html) [26]. Molecular docking between the TLR4 receptor and the multiepitope vaccine construct was performed using the GRAMM docking online program (https://gramm.compbio.ku.edu/gramm) [33]. The docking complex was then visualized and edited using the PyMol molecular graphics system and Discovery Studio Visualizer. In addition, the docking results were further validated using PyMOL. Residue interaction analysis of docking complexes with TLR4 was performed using PDBsum Generate. The docking complex residue interaction data were also compared with the ligand binding site found on the TLR4 receptor. TLR4 ligand binding site map can be determined by analysis using PRANKWEB (https://prankweb.cz) [34]. Based on the analysis using PRANKWEB, several binding sites, referred to as pockets, were identified, along with the corresponding amino acid residues and the probability of binding at these sites.

Molecular dynamics

Molecular dynamics analysis was performed by submitting the PDB files of the multiepitope vaccine construct, TLR4 receptor, and their complex into the online program CABS-Flex 2.0 (http://biocomp.chem.uw.edu.pl/CABSflex2) [35]. Default mode settings (minimum restraint, 38; maximum restraint, 8.0; gap, 3; SS mode; temperature, 1.4) were used in the molecular dynamics analysis using CABS-Flex 2.0. The results of the analysis will determine the flexibility of the vaccine based on structural heterogeneity, optimum free energy, and the most stable configuration. CABS-Flex 2.0 utilizes the coarse-grained (CG) method for molecular dynamics simulations. In comparison to the all-atom (AA) approach, the CG method offers several advantages, such as being computationally less expensive, well-suited for large biomolecular systems, and significantly reducing running time [36].

Codon optimization and in silico cloning

Codon optimization was performed in order to optimize the expression of the protein sequences. Codon optimization was performed *in silico* using the online program JCat (http://www.jcat.de/) [37]. In the codon optimization process, *Escherichia coli* (Strain K12) was chosen as the host for multiepitope vaccine protein expression, and several parameters were selected that should be avoided, including rho-independent transcription termination, prokaryotic ribosome binding sites, and restriction enzyme cutting sites [21]. The *E. coli* K-12 strain was selected as the expression system due to its recognition by the U.S. FDA as safe, its ease of genetic manipulation, and its capability for large-scale protein production [38]. Furthermore, the JCat tool server utilizes *E. coli* K-12 sub-strain MG1655 as one of its reference datasets, which by default directs the optimization process toward this species [37].

After codon optimization, *in silico* cloning was performed by inserting the multiepitope vaccine sequences into the SnapGene software tool [39]. During in silico cloning, the multiepitope vaccine construction sequences were first analyzed for restriction enzyme sites to predict the presence of these sites in the vaccine construction. Restriction enzyme site analysis was performed using the Takara Cut-Site Navigator program (https://www.takarabio.co.jp/research/enzyme/enzyme_search.php). Then, cloning was accomplished by inserting the vaccine construction sequences, which had been modified with restriction enzyme sequences in the N- and C-terminal parts, into the pET-28b(+) vector.

■ RESULTS AND DISCUSSION

TM and CA Immunogenic Protein Sequence Data

The TM protein comprises a 1,077 bp nucleotide sequence that encodes 359 amino acids, resulting in a molecular weight of approximately 41.08 kDa [12]. The CA protein has a 1,164 bp nucleotide sequence encoding 226 amino acids, with a molecular weight of

approximately 25.28 kDa [5]. The sequence data of the immunogenic TM protein are presented in Table 1.

In this study, the TM and CA proteins of the Jembrana disease virus (JDV) were selected as vaccine targets due to their conserved immunogenic epitopes, which have been shown to elicit antibodies in JDV-infected animals. Importantly, the immunogenicity of the TM protein remains intact despite undergoing glycosylation during infection in cattle [40]. Likewise, the CA protein contains several linear and conformational epitopes recognized by antibodies [2]. These characteristics make TM and CA promising components for the development of multiepitope vaccines.

B and T Cell Epitope Analysis Data on TM and CA Proteins of Jembrana Virus Tabanan Strain 1987

During epitope mapping analysis of TM and CA proteins, more than 10 sequences of amino acid epitopes from LBL, CTL, and HTL epitopes were detected. However, from all these epitopes, only 2 epitopes from each epitope were selected for vaccine construction. The selected epitope must fulfill the following requirements: LBL epitope has a length of about 5–8 amino acids, CTL epitope has a length of about 8–11 amino acids [41], HTL epitope has a length of about 13–17 amino acids [9]. The amino acid sequence data for each epitope are presented in Table 2.

Table 1. Nucleotide and amino acid sequences of the TM and CA proteins of the Jembrana disease virus

Protein	Nucleotide sequence	Amino acid sequence
TM	GCCGTGGGGATGGTCATATTCCTTCTCGTGTTAGCTATCA	AVGMVIFLLVLAIMAMTASVTAA
	TGGCGATGACAGCATCTGTCACCGCAGCTGCTACGCTCG	ATLVKQHATAQVVGRLSTNLTYI
	TGAAGCAACACGCCACGGCACAAGTAGTGGGGAGACTGA	TKIQNQYLHLFQNLNTRVNNLHH
	GCACGAATCTAACTTATATCACTAAGATACAGAATCAATA	RVTYLEFLAEVHEVQTGLGCVPR
	CCTGCACCTGTTTCAAAATCTGAACACACGAGTTAATAAT	GRYCHFDWRPEEVGLNMTLWNS
	CTACATCATAGGGTTACTTACCTTGAGTTTTTGGCAGAAG	TTWQQWMSYYDQIEENIWNLKY
	TCCATGAGGTACAAACTGGGCTAGGGTGTGTGCCGAGAG	NWSEALEKGKSNTDGLEPDVFRY
	GAAGATATTGCCATTTTGACTGGCGCCCAGAGGAGGTAG	LADLSSSFTWGSWVDKLVWLAYI
	GATTAAACATGACGCTCTGGAATTCTACCACCTGGCAACA	LLAYFAFKVLQCIMSNLGAQTRY
	ATGGATGTCCTACTACGATCAGATAGAAGAAAACATATG	QLLNAQEDTDPAGDGDQPDDHR
	GAATTTGAAATACAATTGGTCTGAGGCCTTAGAGAAAGG	SGDTPRSGVPSGGWSQKLSEGKKI
	AAAGAGTAATACTGACGGTTTGGAGCCGGATGTCTTCCG	GCLILRTEWQNWRNDLRTLRWLT
	ATACTTGGCAGACCTATCCTCCAGTTTTACATGGGGTAGT	LGGKILQLPLSLLVLLVRILLHILSP
	TGGGTGGATAAGCTTGTATGGCTAGCTTATATACTTTTGG	TFQNQRGWTVGRKGTGGDDREL
	CTTATTTTGCATTTAAGGTCCTCCAGTGCATCATGTCAAA	SPELEYLSWTGSSQEMVEMRDLKE
	CTTGGGCGCTCAAACACGGTATCAGTTGCTGAATGCGCA	EDIPEEGIRPVEM
	AGAGGATACCGACCCTGCAGGGGACGGAGACCAGCCAGA	
	CGACCACCGATCCGGAGACACCCCTCGTTCTGGGGTACC	
	CTCCGGGGGCTGGTCTCAGAAGCTCAGCGAAGGCAAGAA	
	GATCGGATGTCTGATCTTGAGAACAGAATGGCAGAATTG	
	GAGGAACGATTTGAGGACCTTGCGCTGGTTGACTCTGGG	
	GGGAAAAATCCTGCAGCTCCCGCTCAGTCTGTTAGTCCTC	
	CTAGTTCGAATCCTTTTGCATATTCTCTCTCCCACTTTTCA	
	AAATCAAAGAGGGTGGACTGTGGGGAGAAAGGGAACAG	
	GTGGGGACGACCGGGAGCTTTCCCCGGAGCTGGAATATC	
	TGAGTTGGACTGGATCGAGTCAGGAGATGGTGGAGATGA	
	GAGACCTAAAGGAGGAAGATATCCCCGAGGAGGGAATAC	
	GCCCAGTTGAGATG	
CA	CCTCAGCTGAGAAAGAACTTCCCCGCCGTGAGCACCTCC	PQLRKNFPAVSTSDGSPRYDPDLT
	GACGGCTCTCCTAGATACGACCCCGACCTGACCAAGCAG	KQLKIWADATEKHGVDHHAVNI

Protein	Nucleotide sequence	Amino acid sequence
	CTGAAGATTTGGGCCGACGCCACCGAGAAGCACGGCGTG	LGVITANLTQSEIRLLLQSTPQWRL
	GATCACCACGCCGTGAACATCCTGGGCGTGATCACCGCC	DIQLIESKLNAREHAHRVWKESHP
	AACCTGACCCAGAGCGAGATCCGGCTGCTGCTGCAGAGC	EAPKTDEIIGKGLTAAEQATLTTQ
	ACCCCCCAGTGGAGGCTGGACATCCAGCTGATCGAGTCC	ECRDTYRQWVLEAALEVAQGKH
	AAGCTGAACGCCCGGGAGCACGCCCACAGAGTGTGGAAG	DRPGPINIHQGPKEPYPEFVNKLV
	GAGAGCCACCCCGAGGCCCCTAAGACCGACGAGATCATC	TALEGMAAPETTKQYLLDHLSVD
	GGCAAGGGCCTGACCGCCGCCGAGCAAGCTACCCTGACC	HANEDCRAVLLPLGPSAPMERKLE
	ACCCAAGAATGCCGCGACACCTACCGCCAGTGGGTGCTG	ACRAVGSSKQKMQF
	GAGGCCGCTCTGGAAGTGGCCCAAGGCAAGCACGACCGG	
	CCCGGACCTATCAACATCCACCAAGGCCCCAAGGAGCCC	
	TACCCCGAGTTCGTGAACAAGCTGGTGACCGCCCTGGAG	
	GGCATGGCCGCTCCTGAAACCACCAAGCAGTACCTGCTG	
	GACCACCTGAGCGTGGACCACGCCAACGAGGACTGCCGG	
	GCTGTGCTGCTGCCCCTGGGACCTTCTGCCCCTATGGAGC	
	GGAAGCTGGAGGCCTGCCGCGCTGTGGGAAGCTCTAAGC	
	AGAAGATGCAGTTC	

Table 2. The amino acid sequence of the TM and CA protein epitope

Protein	Cytotoxic T lymphocyte (CTL) epitope	Helper T lymphocyte (HTL) epitope	Linear B lymphocyte (LBL) epitope
TM	KQHATAQVVTKIQNQYLH	AVGMVIFLLVLAIMAAMTASVTAAATLVKQ	ALEKGKSNRDLKEEDIP
CA	LQSTPQWRLIHQGPKEPY	STSDGSPRYDPDLTKLGVITANLTQSEIRL	SDGSPRYDPDLTKQESHPEAPKT

Three complementary prediction methods were applied to identify the most promising B-cell epitopes from these proteins, such as BepiPred Linear Epitope Prediction 2.0, Emini Surface Accessibility Prediction, and Kolaskar & Tongaonkar Antigenicity. BepiPred 2.0, which uses a random forest algorithm based on decision trees, was employed to predict linear epitopes with high accuracy [42]. The Emini Surface Accessibility Prediction was then used to determine whether predicted epitopes are likely to be exposed on the protein surface [43], while the Kolaskar & Tongaonkar Antigenicity assessment evaluated their physicochemical properties to estimate antigenicity [44]. The overlap in predictions from these methods reinforces the reliability of the identified epitopes, increasing confidence in their potential to elicit strong B-cell responses.

To complement B-cell targeting, cytotoxic T lymphocyte (CTL) and helper T cell (HTL) epitopes were predicted to ensure a balanced humoral and cellular immune response. CTL epitopes were identified using the IEDB TepiTool with the BoLA-D18.4 MHC class I allele, a well-characterized bovine allele that has been previously used for other veterinary vaccine targets [45]. HTL epitopes were predicted using the NetBoLAIIpan tool, which employs a pan-specific approach to cover BoLA-DRB3 alleles prevalent in cattle [46]. Together, these predictions ensure that the vaccine construct has the potential to activate both CD8+ and CD4+ T cell pathways, enhancing overall immune protection.

Multiepitope Vaccine Construct

In the design of the Jembrana disease multiepitope vaccine, the selected TM and CA protein epitopes were arranged consecutively, starting from the N-terminal adjuvant TLR4 agonist ribosomal 50S L7/L12, CTL epitope connected with AAY linker, HTL epitope connected with KK linker, LBL epitope connected with GPGPG linker. In this study, 12 epitopes were used, with a total of 309 amino acid residues in the vaccine construction. The arrangement of each component in the multiepitope vaccine construction is shown in Fig. 1.

The 50S L7/L12 ribosomal protein sequence, a known TLR4 agonist, was included as an adjuvant to stimulate antigen-presenting cells (APCs) and induce

proinflammatory cytokines such as TNF-α, IL-1β, and IL-6 [47]. This strategy is supported by evidence that TLR4 activation can significantly boost both innate and adaptive immune responses. Additionally, the construct utilized a combination of rigid and flexible linkers to optimize structural stability and epitope presentation. The rigid EAAAK linker stabilizes the construct via α-helix formation [48], while flexible linkers such as AAY, GPGPG, and KK improve flexibility and immune accessibility [49]. Notably, GPGPG linkers have been shown to enhance CD4+ T cell responses [50], and KK linkers help reduce immunodominance at junctional epitopes [51].

The choice and arrangement of linkers had a direct impact on the secondary structure of the construct. AAY linkers, rich in alanine, promoted α-helix formation [52], while GPGPG linkers, containing glycine and proline, contributed flexibility and loop formation [53]. Conversely, KK linkers favored random coil structures over α-helices [54]. Structural modeling revealed that the construct exhibited a high α-helix content, providing the 50S L7/L12 ribosomal protein sequence, a known TLR4 agonist, was included as an adjuvant to stimulate antigen-presenting cells (APCs) and induce proinflammatory cytokines such as TNF-α, IL-1β, and IL-6 [47]. This strategy is supported by evidence that TLR4 activation can significantly boost both innate and adaptive immune responses. Additionally, the construct utilized a combination of rigid and flexible linkers to optimize structural stability and epitope presentation. The rigid EAAAK linker stabilizes the construct via α-helix formation [48], while flexible linkers such as AAY, GPGPG, and KK improve flexibility and immune accessibility [49]. Notably, GPGPG linkers have been shown to enhance CD4+ T cell responses [50], and KK linkers help reduce immunodominance at junctional epitopes [51].

The choice and arrangement of linkers had a direct impact on the secondary structure of the construct. AAY linkers, rich in alanine, promoted α-helix formation [52], while GPGPG linkers, containing glycine and proline, contributed flexibility and loop formation [53]. Conversely, KK linkers favored random coil structures over α-helices [54]. Structural modeling revealed that the construct exhibited a high α-helix content, providing a robust framework [55], a low β-sheet content, which reduces aggregation risks [56], and a mix of β-turns and random coils that may enhance epitope exposure to the immune system [57].

Secondary Structure and 3D Structure Prediction

Furthermore, the secondary structure was analyzed from this construction, and then the 3D structure was modeled. In this study, five models were obtained, and model 1 was selected for further validation. Model 1 was chosen because it was more accurate and robust. The secondary structure is illustrated in Fig. 2, while the 3D structure is shown in Fig. 3.

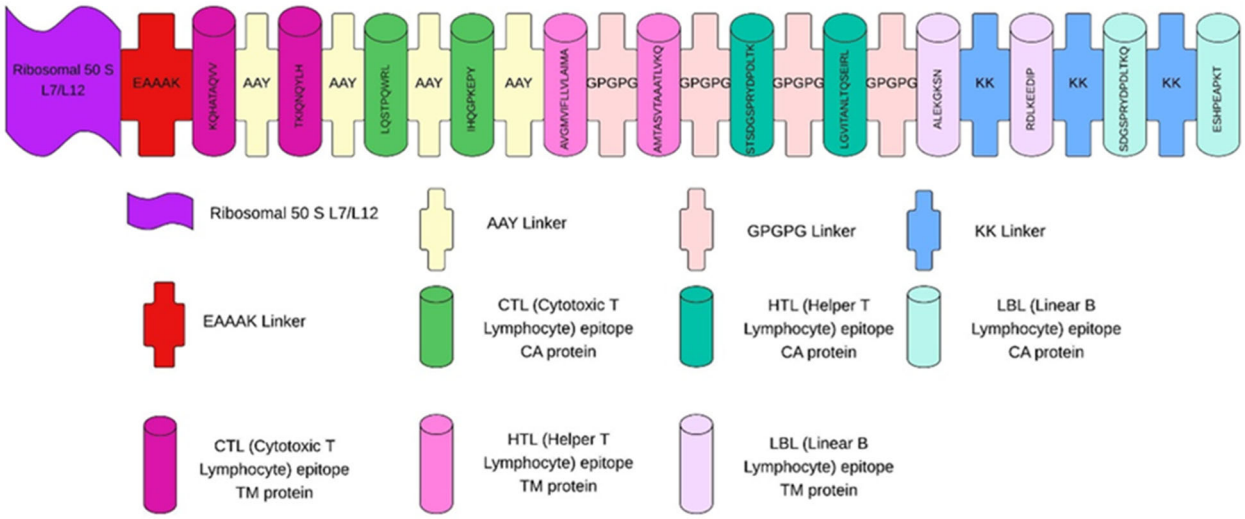

Fig 1. Jembrana disease multiepitope vaccine construct

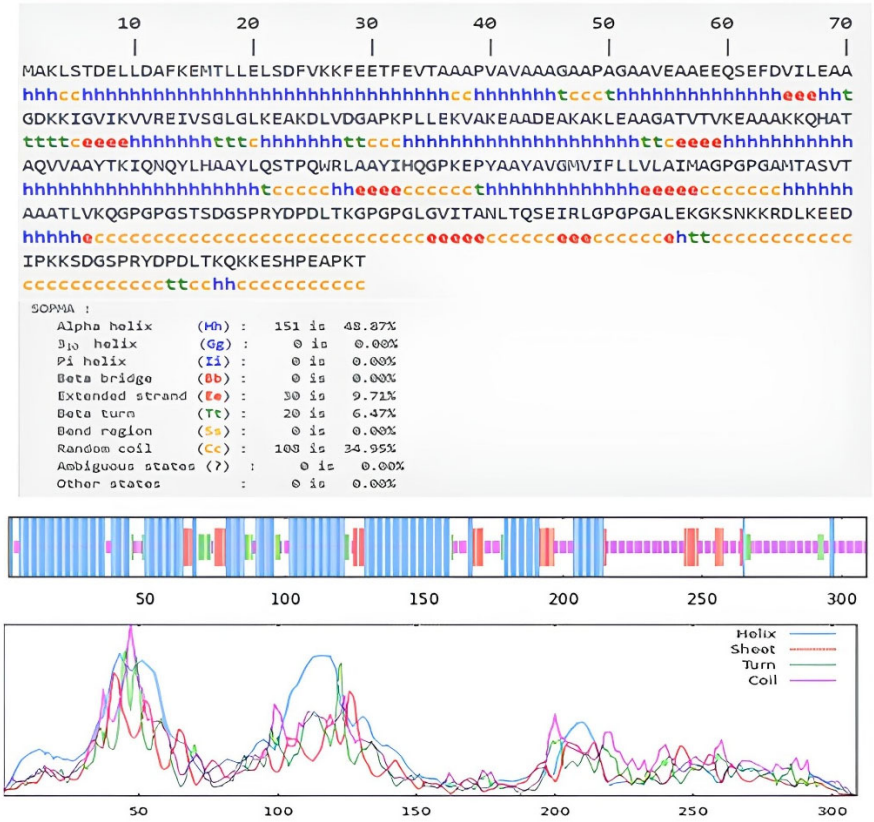

Fig 2. Prediction of the secondary structure of the multiepitope vaccine construct

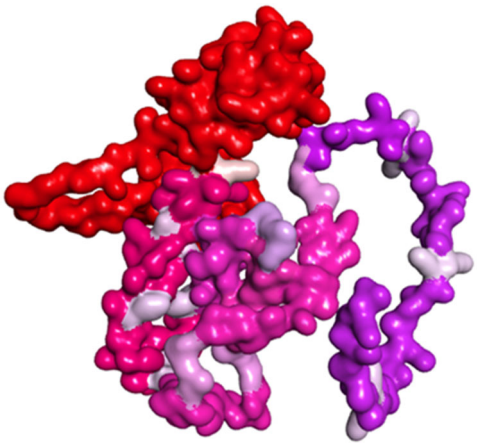

Fig 3. 3D model of multiepitope vaccine construct. Based on the colors, the red is TLR4 agonist ribosomal 50S L7/L12 adjuvant, light red is EAAAK linker, pink is epitope CTL, light pink is AAY linker, magenta is epitope HTL, light magenta is GPGPG linker, purple is epitope LBL, and light purple is KK linker

In Fig. 2, the secondary structure of the multiepitope vaccine consists of 48.87% α-helix, 9.71% extended strands associated with β-sheet formation, 6.47% β-turns, and 34.95% random coils. The α-helix is predominantly present in the TLR4 agonist ribosomal 50S L7/L12 adjuvant, all CTL epitopes, the HTL epitope of the TM protein, and three residues of the LBL epitope at positions 256, 297, and 298. Extended strands were identified at residues 65–67, 86–89, 136–139, 169–172, 193–197, 216, 235–239, 256–258, and 266. The β-turns were identified at residues 46, 50, 70–74, 87–89, 98–99, 123–124, 161, 179, 267–268, and 293–294. Random coil structures were mainly present in the adjuvant region (residues 4–5, 37–38, 47–49, 75, 80, 90–92, and 125), in parts of the CTL epitope from the CA protein (residues 163–167 and 173–178), and in most HTL and LBL epitopes.

Analysis of Quality and Validation

Multiepitope vaccine structures were verified using the ERRAT program. The principle of ERRAT is to analyze the non-bonded atom-atom interaction in a protein structure and compare it with a database of high-resolution and reliable structures. The results of

structure verification using ERRAT are shown in Fig. 4. Based on the ERRAT verification results shown in Fig. 4, the model exhibited an overall quality score of 95.098 with an error rate of less than 5%, indicating that the structure can be categorized as reliable. ERRAT scores above 90% generally indicate that the majority of non-bonded interactions in the model fall within the acceptable range observed in experimentally determined protein structures. The low error rate (< 5%) in this model suggests that the atomic interaction geometry closely resembles that of well-resolved protein structures [25].

Furthermore, according to the Ramachandran plot in Fig. 5, generated using the PDBsum analysis program, 94.2% of residues are located in the most favored region, 4.6% in the additionally allowed region, 1% in the generously allowed region, and 0% in the disallowed region. The analysis confirmed that the vaccine is stable and reliable, with 94.2% of residues located in the most favored regions and no residues in disallowed regions. Analysis of the amino acid distribution on the Ramachandran plot reveals that, in general, the amino acids adopt anti-parallel β-sheet, parallel β-sheet, and left-handed α-helix structures. Notably, two amino acids (Glu301 and Lys136) are located in the generously allowed region, while one amino acid (Ser270) does not adopt a defined structure as it is positioned in quadrant 4 of the Ramachandran plot.

Physiochemical Analysis, Allergenicity, Antigenicity, and Toxicity of Multiepitope Vaccine Constructs

In addition to its structural quality, the vaccine construct has a molecular weight of 32.292 kDa, which indicates ease of purification [58-59]. Its stability is supported by an instability index of 29.32, which classifies it as stable [60], and its thermostability is confirmed by an aliphatic index of 85.44. The secondary structure composition, with 6.47% beta turns and 34.95% random coils, contributes to a flexible spatial arrangement that facilitates effective epitope formation. According to ProtParam analysis, the estimated half-life of the construct is 30 h in mammalian reticulocyte cells (*in vitro*), more than 20 h in yeast (*in vivo*), and over 10 h in *E. coli* (*in vivo*).

Beyond structural integrity, the construct also demonstrated favorable immunological safety. Computational predictions consistently identified it as antigenic, non-allergenic, and non-toxic—key properties of a viable vaccine candidate. Antigenicity ensures

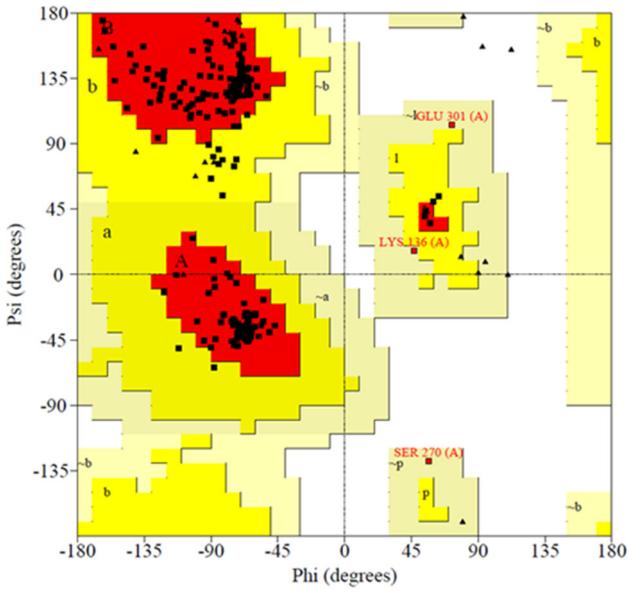

Fig 5. Ramachandran plot of multiepitope vaccine constructs. "Red" regions indicate the "most favored region", "light yellow" regions indicate the "additionally allowed" region, "pale yellow" regions indicate the "generously allowed" region, and "white" regions indicate the "disallowed" region

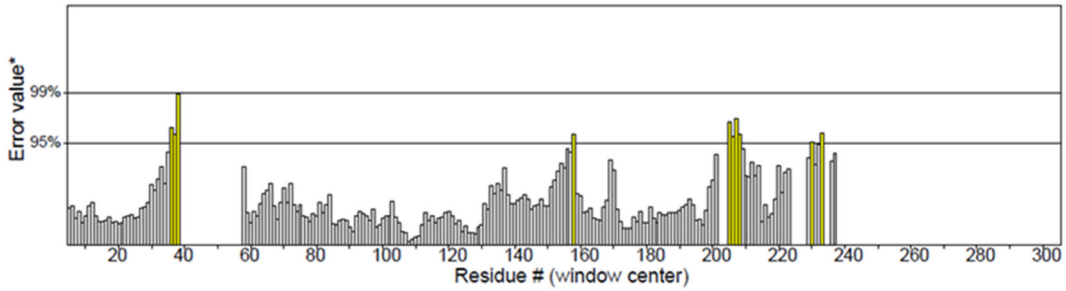

Fig 4. Verification of multiepitope vaccine constructs. The yellow-colored part is the 95% rejected part of the structure

stimulation of B and T cell responses [60], non-allergenicity minimizes the risk of hypersensitivity [61], and non-toxicity guarantees compatibility with host tissues [62]. These findings were further validated by specialized tools. Allergenicity analysis using AllerTOP v.2.0 classified the construct as non-allergenic, while VaxiJen v2.0 predicted an antigenicity score of 0.4986, exceeding the 0.4 threshold and confirming its antigenic nature. In addition, ToxIBTL analysis indicated that the construct is non-toxic. These combined features suggest that the construct can effectively interact with immune receptors without eliciting harmful side effects.

Molecular Docking Between the Vaccine Construct and TLR4

Since no specific receptor has been identified for Jembrana virus infection, this study utilized the TLR4 receptor as a universal receptor, known to bind to ENV proteins, to evaluate the interaction capability between the receptor and the vaccine through molecular docking [39]. Molecular docking was performed by interacting the TLR4 of *B. indicus*, which serves as a receptor, and a multiepitope vaccine construct, which acts as a ligand, using the GRAMM program. The results obtained from molecular docking were several possible complexes formed between TLR4 and the multiepitope vaccine construct, with the lowest interaction energy value recorded at −66 kcal/mol. Furthermore, the docking analysis yielded a root mean square deviation (RMSD) value of 0.442 Å, which indicates a highly reliable and stable docking pose. Previous studies have reported that docking models with sub-angstrom RMSD values (< 1 Å) are categorized as high-quality, accurately reproducing experimental structures and thereby validating the docking results obtained in this study [41].

The docking complex was also analyzed for the interaction between residues using PDBsum Generate, which resulted in three types of interactions: three salt bridges, eight hydrogen bonds, and 459 non-bonded contacts. The binding site of the ligand (multiepitope vaccine construct) to the TLR4 receptor, as well as the binding probability between the TLR4 receptor and the multiepitope vaccine construct, is illustrated in Fig. 6.

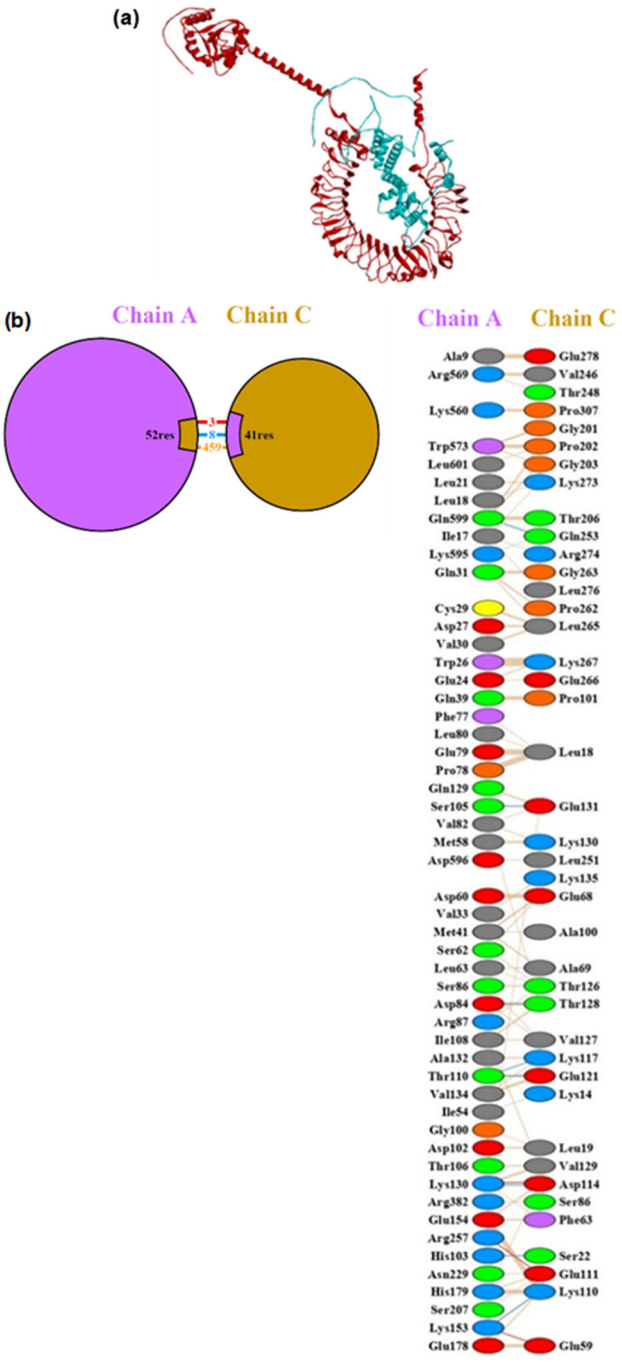

Fig 6. (a) 3D visualization of molecular docking between TLR4 of Bos indicus with Jembrana disease virus multiepitope vaccine construct, "red structure" indicates receptor, "turquoise structure" indicates multiepitope vaccine construct. (b) Interactions between residues in the docking complex: "red line" indicates salt bridge, "blue line" indicates hydrogen bond, "orange dashed line" indicates non-bonded contact

Based on Fig. 6, it can be seen that there were three types of interactions: three salt bridges, seven hydrogen bonds, and 453 non-bonded contacts. A salt bridge occurs between residues Lys130, Lys153, and Arg257. Hydrogen bonds occur on residues: Asp84, His103, Ser105, Thr110, Lys130, Lys153, and Gln599. Non-bonded contact itself is an interaction between atoms that are not connected by covalent bonds [63]. In this case, a non-covalent bond refers to bonds other than ionic bonds and hydrogen bonds, such as van der Waals interactions and hydrophobic bonds.

In Table 3, it can be seen that the vaccine construct can interact with the ligand binding site on TLR4 through two types of interactions: specifically, hydrogen bonds

Table 3. TLR4 ligand binding site map and binding probability of ligand (vaccine construct) on TLR4 receptor

Pocket rank	Position	Score	Probability score	Amino acid	Amino acid number												TLR4+Multi-epitope vaccine construct
1	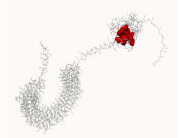	10.15	0.587	12	661	664	665	668	720	724	729	754	757	758	761	762	Gln599 Ser105 Asp84 Thr110 Lys130
2	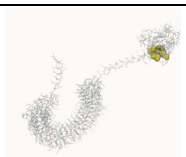	3.61	0.141	9	681	683	709	713	719	745	747	748	751				Lys130 Arg257 His103 Lys153 Lys153
3	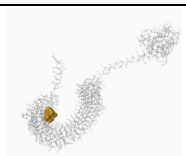	1.61	0.025	6	41	60	62	63	84	86							
4	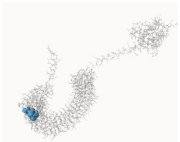	1.36	0.016	6	114	117	136	137	138	144							
5		1.15	0.010	6	771	775	780	787	790	795							
6	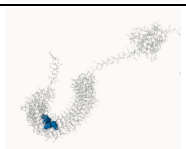	1.08	0.009	6	181	183	209	211	212	263							
7	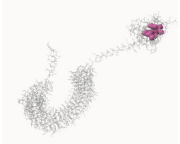	1.06	0.008	6	673	729	731	732	758	764							
8	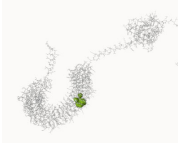	0.84	0.004	5	412	414	429	434	443								

and non-bonded contacts, with a probability of 0.025 (2.5%). The residues that interact in the binding site of the TLR4 receptor are Met41, Asp60, Ser62, Leu63, Asp84, and Ser86. Additionally, the vaccine construct interacts with TLR4 outside of the binding pocket, forming salt bridges (Lys130, Lys153, and Arg257), hydrogen bonds (Asp84, His103, Ser105, Thr110, Lys130, Lys153, and Gln599), and non-bonded contacts. The presence of hydrogen bonds and strong ionic bonds suggests a close and stable interaction between the vaccine construct and TLR4 [21].

Molecular Dynamics Between Vaccine Constructs and TLR4

To determine the stability of the multiepitope vaccine construct's structure, molecular dynamics simulations were performed on the docking complex with the minimum binding energy, the non-interacting vaccine construct, and the non-interacting TLR4. The simulation results of molecular dynamics in this study are based on the root mean square fluctuation (RMSF) of the docking complex, which was then compared with the structure of the non-interacted vaccine construct and TLR4. In this study, molecular dynamics simulations were performed for 50 cycles, with 50-frame trajectories recorded over a 10-ns time period. The RMSF value of the molecular dynamics simulation results for the TLR4 receptor is shown in Fig. 7.

The stability of TLR4 (chain A) was evaluated based on the RMSF values, where the RMSF of the ligand-bound TLR4 receptor was lower than that of the native receptor. As shown in Fig. 7, a total of 341 residues exhibited lower RMSF values. Among these, one residue, Met41, was located within the binding site, resulting in an RMSF decrease from 0.689 to 0.652 Å. In addition, fifteen residues located in interaction regions outside the binding site also displayed decreased RMSF values, including Ile54 (2.338 to 1.958 Å), Met58 (0.444 to 0.441 Å), Phe77 (1.299 to 1.191 Å), Gly100 (1.204 to 0.707 Å), His103 (0.853 to 0.833 Å), Ser105 (0.644 to 0.462 Å), Gln129 (0.501 to 0.293 Å), Val134 (0.483 to 0.449 Å), Lys153 (0.791 to 0.409 Å), Glu154 (0.410 to 0.246 Å), Glu178 (0.458 to 0.335 Å), His179 (0.417 to 0.103 Å), Lys595 (0.677 to 0.346 Å), Asp569 (2.287 to 1.732 Å), and Asp596 (0.767 to 0.471 Å). Although only one residue within the binding site exhibited a reduction in RMSF value, the observed decreases in other regions may also contribute to the overall stability of the receptor [64].

The stability of the vaccine was evaluated based on RMSF values. The RMSF of the vaccine (chain C) in complex with TLR4 was lower than that of the unbound vaccine, indicating reduced structural flexibility upon interaction. As shown in Fig. 8, a total of 118 residues exhibited lower RMSF values in the vaccine–TLR4 complex compared to the unbound form. Among these, three residues were located in the TLR4 ligand-binding site, such as Glu68 (from 0.501 to 0.641 Å), Ala69 (from 0.787 to 0.826 Å), and Ala100 (from 1.319 to 1.593 Å). In addition, 17 residues located outside the binding site but still involved in interaction also showed decreased RMSF values, including Glu59 (from 2.743 to 2.129 Å),

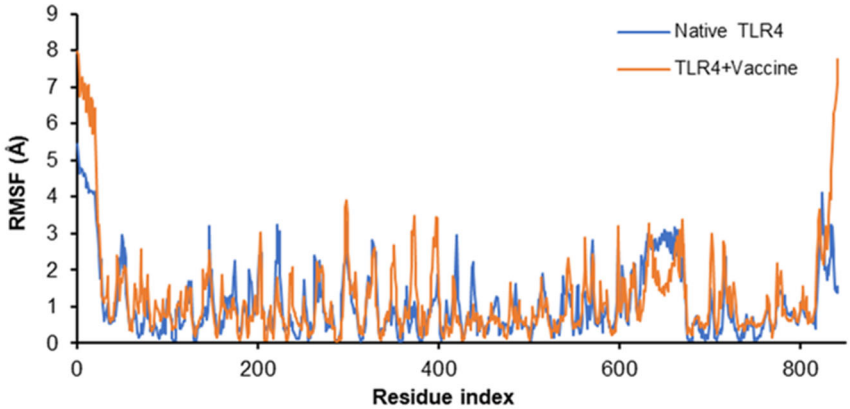

Fig 7. Comparative graph of RMSF between the docked TLR4 receptor with vaccine construct (blue line) and native TLR4 receptor (orange line)

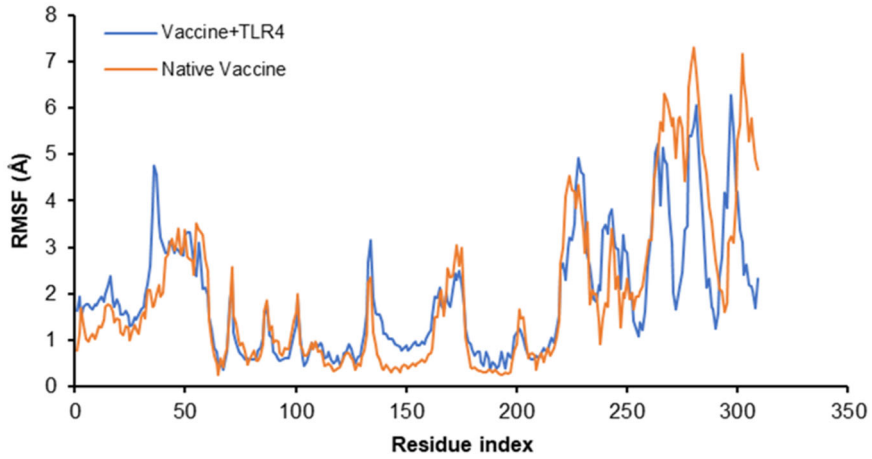

Fig 8. Comparative RMSF graph between vaccine constructs docked with TLR4 receptor (blue line) and native vaccine (orange line)

Ser86 (from 1.628 to 1.513 Å), Pro101 (from 1.992 to 1.891 Å), Gly201 (from 1.654 to 1.245 Å), Pro202 (from 1.458 to 1.179 Å), Gly203 (from 1.484 to 1.037 Å), Thr206 (from 0.683 to 0.599 Å), Gln253 (from 1.656 to 1.405 Å), Pro262 (from 4.477 to 4.322 Å), Leu265 (from 5.693 to 3.906 Å), Glu266 (from 5.505 to 5.143 Å), Lys267 (from 6.314 to 4.894 Å), Lys273 (from 5.756 to 1.984 Å), Arg274 (from 5.800 to 2.167 Å), Leu276 (from 4.435 to 3.370 Å), Glu278 (from 6.435 to 5.391 Å), and Pro307 (from 5.424 to 2.037 Å). Overall, the lower RMSF values were predominantly distributed across the epitope regions, suggesting that the epitope structures remain stable, thereby indicating a high potential for interaction with MHC molecules or immune system receptors [65].

Codon Optimization and *In Silico* Cloning of Multiepitope Vaccine Construct

The multiepitope vaccine construct, after codon optimization, consists of 309 amino acids and 927 nucleotides. The optimized sequence achieved a Codon Adaptation Index (CAI) of 1.0, which falls within the ideal CAI range of 0.9 to 1.0 [37]. In *E. coli* samples, higher CAI values showed a positive linear correlation with protein expression levels, indicating that genes with elevated CAI values tend to be expressed more efficiently [66]. In addition to the CAI value, the GC content of a gene also influences protein expression in the *E. coli* expression system. Extremely low GC content (< 30%) or excessively high GC content (> 80%) should be avoided, as both can reduce mRNA stability and interfere with translation initiation [67]. In this study, codon optimization resulted in an overall GC content of 51.99%, which falls within the moderate range of GC content.

In order to evaluate the simulation of inserting vaccine constructs into expression vectors, an *in silico* cloning process was performed in this study. This approach also provides insights into protein expression in the *E. coli* BL-21 (DE3) prokaryotic system. The pET 28b+ vector was used as the prokaryotic cloning vector in this study. The *E. coli* BL21 (DE3) strain was selected due to its widespread use in recombinant protein production. For the *in silico* cloning process, restriction enzyme sites XhoI and NdeI were added to the N- and C-terminal regions of the construct, respectively. The results of this cloning simulation are presented in Fig. 9.

Based on Fig. 9, the pET-28b(+) plasmid has a length of 5,368 bp. After the addition of the multiepitope vaccine construct, which includes XhoI and NdeI restriction enzyme sites and has a length of 939 bp, the total sequence length of the plasmid is approximately 6223 bp. Previous studies have shown that pET-28b(+)-based expression systems can successfully produce multiepitope proteins of various sizes, including brucellosis diagnostic proteins < 65 kDa [68] and HIV envelope-derived constructs 32 and 53 kDa [69]. Based on these findings, it is possible that the Jembrana virus multiepitope vaccine protein could also be efficiently

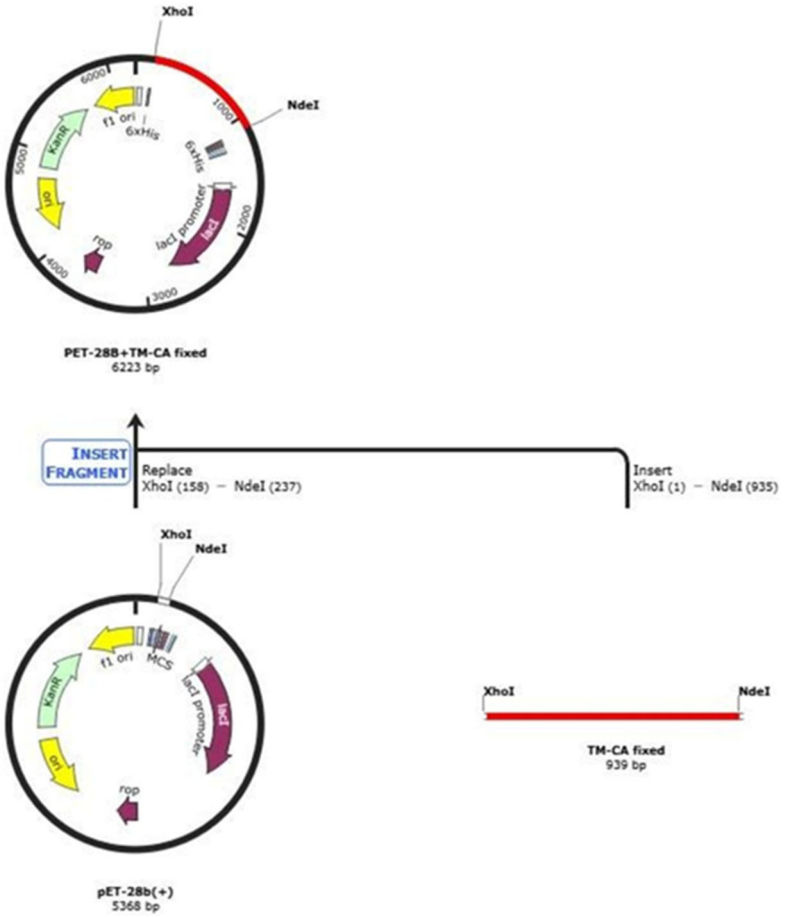

Fig 9. *In silico* cloning of multiepitope vaccine in pET-28b (+) plasmid

expressed in the *E. coli* BL21 system, providing a practical platform for large-scale production.

Immune Simulation Analysis

Immune simulation analysis is a crucial step in the development of multiepitope vaccines, as it enables the evaluation of their ability to induce immune responses [70]. The results of the immune simulation are shown in Fig. 10. The immune response simulation of the multiepitope vaccine construct is presented in Fig. 10. Antigen levels increased following vaccine administration on days 1, 14, and 28, while antibody production rose significantly after the first booster (day 15) and continued to increase until day 35. B-cell populations expanded accordingly, with IgM isotypes observed in the early phase and IgG1 and IgG2 appearing after day 15, steadily rising until day 30. CD4+ T-helper cells also showed a progressive increase, whereas CD8+ cytotoxic T cells peaked shortly after vaccination but gradually declined, suggesting that highly functional antigen-specific CD8+ T cells are not maintained in the long term [71].

Cytokine analysis revealed elevated IFN-γ levels during the early vaccination phase, consistent with the activity of CD8+ T cells, which are known producers of IFN-γ [72]. IL-2 concentrations also increased, corresponding to the proliferation of T-helper cells. Dendritic cells were activated post-vaccination, with antigen-engulfing cells peaking on days 4–5 and again after booster doses. Antigen-presenting dendritic cells via MHC class I increased shortly after vaccination and boosters, while MHC class II presentation remained elevated throughout the study period. Collectively, these findings demonstrate that the multiepitope vaccine construct effectively stimulates both humoral and cellular immune responses, supported by antibody production, T-helper proliferation, cytokine secretion,

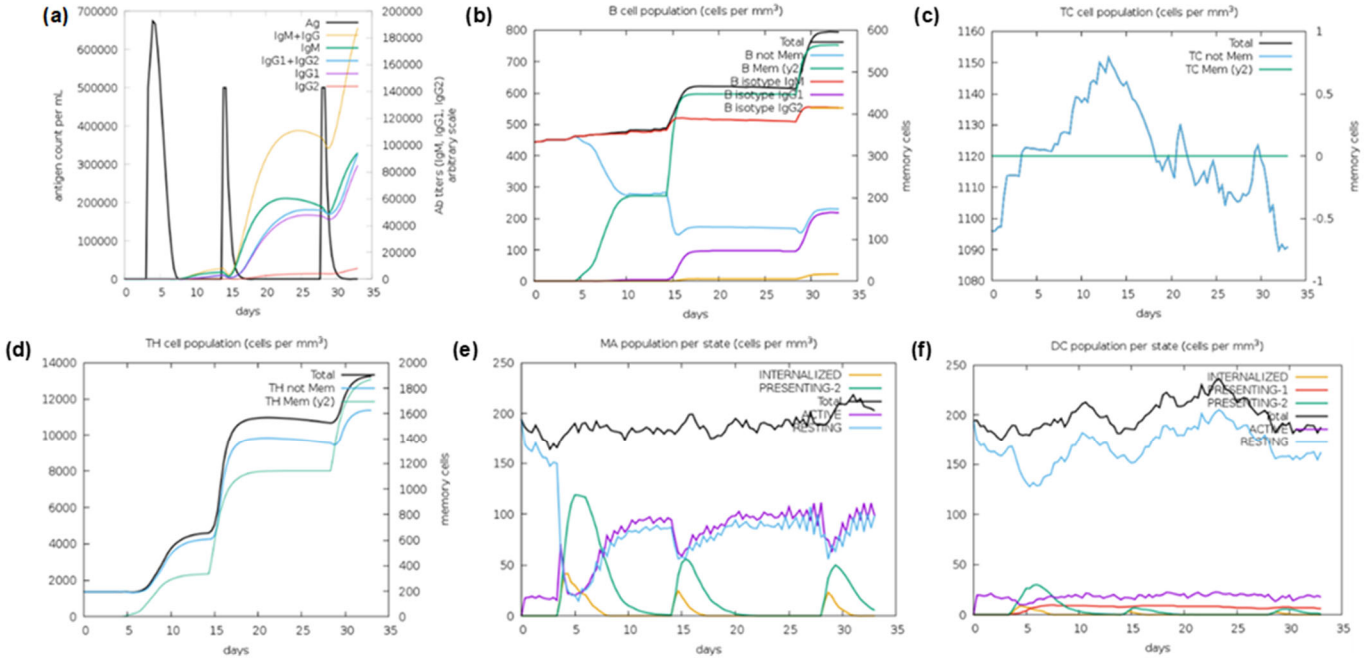

Fig 10. Immune response simulation of the multiepitope vaccine construct. (a) Antibody production, (b) B lymphocyte population after three vaccine administrations, (c) CD8+ cytotoxic T-cell population after injection, (d) CD4+ T-helper population after vaccination, (e) cytokine and interleukin concentrations, and (f) dendritic cell population after vaccination

and dendritic cell involvement. Overall, the integrated computational analysis supports the Jembrana virus multiepitope vaccine construct as a promising candidate for further experimental validation. By combining conserved viral epitopes, immune-enhancing adjuvants, and an expression-ready design, this construct offers a feasible pathway toward developing an effective and scalable JDV vaccine.

■ CONCLUSION

This study successfully designed a multiepitope vaccine candidate against Jembrana disease virus by combining conserved epitopes from the transmembrane and capsid proteins with immune-enhancing adjuvants and optimized linker sequences. *In silico* prediction and validation confirmed the presence of high-probability B-cell, cytotoxic T-lymphocyte, and helper T-lymphocyte epitopes, supporting the potential to induce both humoral and cellular immunity. Structural modeling revealed a stable construct with high α-helix content, low aggregation potential, and optimal epitope exposure, while safety analyses confirmed antigenicity, non-allergenicity, and non-toxicity. Molecular docking and dynamics demonstrated strong and stable binding to the TLR4 receptor, and codon optimization suggested efficient expression in the *E. coli* BL21 (DE3) system. Importantly, immune simulations indicated effective responses, including increased antigen levels, early IgM production followed by IgG1/IgG2 production, expansion of CD4+ T-helper cells, transient CD8+ T-cell activation, elevated IFN-γ and IL-2 levels, and strong dendritic cell involvement via both MHC I and II pathways. Collectively, these findings highlight the vaccine as a promising JDV candidate, and this warrants further validation through *in vitro* and *in vivo* studies.

■ ACKNOWLEDGMENTS

On this occasion, the author would like to express sincere gratitude to the Indonesian Education Scholarship (BPI), the Center for Higher Education Funding and Assessment (PPAPT), the Ministry of Higher Education, Science, and Technology of the Republic of Indonesia, and the Indonesia Endowment Fund for Education (LPDP) for a doctoral scholarship awarded to Fatimah,

under contract number 011927/PPAPT.1.2/BPI.06/02/2025. The author also gratefully acknowledges the RIIM LPDP Grant and the National Research and Innovation Agency (BRIN) for providing research funding support under the *Riset dan Inovasi untuk Indonesia Maju (RIIM)* Program, Batch VII of 2025, in accordance with Decision Number 61/II.7/HK/2024 and Contract Numbers 24/IV/KS/02/2025 and 794/UN1/DITLIT/Dit-Lit/PT.01.03/2025. The author further extends appreciation to the Doctoral Program in Biotechnology, Universitas Gadjah Mada, and the Graduate School of Universitas Gadjah Mada for providing research facilities and support throughout the study period.

■ CONFLICT OF INTEREST

All authors declare no conflicts of interest.

■ AUTHOR CONTRIBUTIONS

Fatimah was responsible for conceptualization, methodology, validation, formal analysis, investigation, data curation, writing the original draft, visualization, and funding acquisition. Syahputra Wibowo contributed to the methodology, validation, and formal analysis, provided resources, and participated in writing, reviewing the draft, editing, and supervision. Dini Wahyu Kartika Sari contributed to reviewing the draft and supervision. Rarastoeti Pratiwi also contributed to reviewing the draft and supervision. Asmarani Kusumawati contributed to reviewing the draft, as well as supervision and project administration. All authors agreed to the final version of this manuscript.

■ REFERENCES

[1] Meles, D.K., Khairullah, A.R., Utama, S., Wurlina, W., Mulyati, S., Mustofa, I., Rimayanti, R., Lestari, T.D., Moses, I.B., Wibowo, S., Wardhani, B.W.K., Kurniasih, D.A.A., Kusala, M.K.J., Ahmad, R.Z., Fauziah, I., Wasito, W., and Akintunde, A.O., 2025, Jembrana disease in Indonesia: An updated review, *Open Vet. J.*, 15 (3), 1091–1100.

[2] Desport, M., Stewart, M., Sheridan, C., Ditcham, W., Setiyaningsih, S., Tenaya, W.M., Hartaningsih, N., and Wilcox, G., 2005, Recombinant Jembrana disease virus gag proteins identify several different antigenic domains but do not facilitate serological differentiation of JDV and nonpathogenic bovine lentiviruses, *J. Virol. Methods*, 124 (1-2), 135–142.

[3] Kusumawati, A., Wanahari, T.A., Astuti, P., Kurniasih, M., Mappakaya, B.A., and Wuryastuty, H., 2015, Vaccine against Jembrana disease virus infection: A summary of findings, *Am. J. Immunol.*, 11 (3), 68–73.

[4] Ditcham, W.G., Lewis, J.R., Dobson, R.J., Hartaningsih, N., Wilcox, G.E., and Desport, M., 2009, Vaccination reduces the viral load and the risk of transmission of Jembrana disease virus in Bali cattle, *Virology*, 386 (2), 317–324.

[5] Unsunnidhal, L., Ishak, J., and Kusumawati, A., 2019, Expression of gag-CA gene of Jembrana disease virus with cationic liposomes and chitosan nanoparticle delivery systems as DNA vaccine candidates, *Trop. Life Sci. Res.*, 30 (3), 15–36.

[6] Lee, J., Arun Kumar, S., Jhan, Y.Y., and Bishop, C.J., 2018, Engineering DNA vaccines against infectious diseases, *Acta Biomater.*, 80, 31–47.

[7] Zhang, L., 2018, Multiepitope vaccines: A promising strategy against tumors and viral infections, *Cell. Mol. Immunol.*, 15 (2), 182–184.

[8] Behmard, E., Abdulabbas, H.T., Abdalkareem Jasim, S., Najafipour, S., Ghasemian, A., Farjadfar, A., Barzegari, E., Kouhpayeh, A., and Abdolmaleki, P., 2022, Design of a novel multiepitope vaccine candidate against hepatitis C virus using structural and nonstructural proteins: an immunoinformatics approach, *PLoS One*, 17 (8), e0272582.

[9] Li, M., Zhu, Y., Niu, C., Xie, X., Haimiti, G., Guo, W., Yu, M., Chen, Z., Ding, J., and Zhang, F., 2022, Design of a multiepitope vaccine candidate against *Brucella melitensis*, *Sci. Rep.*, 12 (1), 10146.

[10] Siddiki, A.Z., Alam, S., Tithi, F.A., Hoque, S.F., Sajib, E.H., Bin Hossen, F.F., and Hossain, M.A., 2023, Construction of a multiepitope *in silico* vaccine against *Anaplasma marginale* using immunoinformatics approach, *Biocatal. Agric. Biotechnol.*, 50, 102706.

[11] Uddin, M.B., Tanni, F.Y., Hoque, S.F., Sajib, E.H., Faysal, M.A., Rahman, M.A., Galib, A., Al Emon, A.,

Hossain, M.M., Hasan, M., and Ahmed, S.S.U., 2022, A candidate multiepitope vaccine against lumpy skin disease, *Transboundary Emerging Dis.*, 69 (6), 3548–3561.

[12] Rahimnahal, S., Yousefizadeh, S., and Mohammadi, Y., 2023, Novel multiepitope vaccine against bovine brucellosis: Approach from immunoinformatics to expression, *J. Biomol. Struct. Dyn.*, 41 (24), 15460–15484.

[13] Riaz, R., Zahid, S., and Khan, M.S., 2024, Designing an epitope-based vaccine against bovine viral diarrhea using immuno-informatics, *Pak. Vet. J.*, 44 (2), 465–475.

[14] Vita, R., Blazeska, N., Marrama, D., IEDB Curation Team Members, Duesing, S., Bennett, J., Greenbaum, J., De Almeida Mendes, M., Mahita, J., Wheeler, D.K., Cantrell, J.R., Overton, J.A., Natale, D.A., Sette, A., and Peters, B., 2025, The immune epitope database (IEDB): 2024 update, *Nucleic Acids Res.*, 53 (D1), D436–D443.

[15] Susianti, S., Bahri, S., Hadi, S., Setiawansyah, A., Rachmadi, L., Fadilah, I., and Ratna, M.G., 2025, Integrating the network pharmacology and molecular docking confirmed with *in vitro* toxicity to reveal potential mechanism of non–polar fraction of *Cyperus rotundus* Linn as anti-cancer candidate, *J. Multidiscip. Appl. Nat. Sci.*, 5 (1), 56–73.

[16] Yogaswara. R., Pranowo, H.D., Prasetyo, N., and Pulung, M.L., 2025, Investigation of new 4-benzyloxy-2-trichloromethylquinazoline derivatives as Plasmodium falciparum dihydrofolate reductase-thymidylate synthase inhibitors: QSAR, ADME, drug-likeness, toxicity, molecular docking and molecular dynamics simulation, *J. Multidiscip. Appl. Nat. Sci.*, 5 (2), 456–486.

[17] Fitria, A., Kurniawan, Y.S., Ananto, A.D., Jumina, J., Sholikhah, E.N., and Pranowo, H.D., 2025, Allyl-modified of calix[4]resorcinarene derivatives for HER2 inhibition agents: An *in silico* study, *J. Multidiscip. Appl. Nat. Sci.*, 5 (2), 352–369.

[18] Ishak, J., Unsunnidhal, L., Martien, R., and Kusumawati, A., 2019, *In vitro* evaluation of chitosan–DNA plasmid complex encoding Jembrana disease virus Env-TM protein as a vaccine candidate, *J. Vet. Res.*, 63 (1), 7–16.

[19] Melchjorsen, J., 2013, Learning from the messengers: Innate sensing of viruses and cytokine regulation of immunity – Clues for treatments and vaccines, *Viruses*, 5 (2), 470–527.

[20] Fisch, A., Reynisson, B., Benedictus, L., Nicastri, A., Vasoya, D., Morrison, I., Buus, S., Ferreira, B.R., Kinney Ferreira de Miranda Santos, I., Ternette, N., Connelley, T., and Nielsen, M., 2021, Integral use of immunopeptidomics and immunoinformatics for the characterization of antigen presentation and rational identification of BoLA-DR-presented peptides and epitopes, *J. Immunol.*, 206 (10), 2489–2497.

[21] Yu, M., Zhu, Y., Li, Y., Chen, Z., Li, Z., Wang, J., Li, Z., Zhang, F., and Ding, J., 2022, Design of a recombinant multivalent epitope vaccine based on SARS-CoV-2 and its variants in immunoinformatics approaches, *Front. Immunol.*, 13, 884433.

[22] Mazumder, L., Hasan, M.R., Fatema, K., Begum, S., Azad, A.K., and Islam, M.A., 2023, Identification of B and T cell epitopes to design an epitope-based peptide vaccine against the cell surface binding protein of monkeypox virus: An immunoinformatics study, *J. Immunol. Res.*, 2023 (1), 2274415.

[23] Jumper, J., Evans, R., Pritzel, A., Green, T., Figurnov, M., Ronneberger, O., Tunyasuvunakool, K., Bates, R., Žídek, A., Potapenko, A., Bridgland, A., Meyer, C., Kohl, S.A.A., Ballard, A.J., Cowie, A., Romera-Paredes, B., Nikolov, S., Jain, R., Adler, J., Back, T., Petersen, S., Reiman, D., Clancy, E., Zielinski, M., Steinegger, M., Pacholska, M., Berghammer, T., Bodenstein, S., Silver, D., Vinyals, O., Senior, A.W., Kavukcuoglu, K., Kohli, P., and Hassabis, D., 2021, Highly accurate protein structure prediction with AlphaFold, *Nature*, 596 (7873), 583–589.

[24] Heo, L., Park, H., and Seok, C., 2013, GalaxyRefine: Protein structure refinement driven by side-chain repacking, *Nucleic Acids Res.*, 41 (W1), W384–W388.

[25] Dym, O., Eisenberg, D., and Yeates, T.O., 2012, ERRAT, *Int. Tables Crystallogr.*, 21, 678–679.

[26] Laskowski, R.A., Jabłońska, J., Pravda, L., Vařeková, R.S., and Thornton, J.M., 2018, PDBsum: Structural summaries of PDB entries, *Protein Sci.*, 27 (1), 129–134.

[27] Gasteiger, E., Hoogland, C., Gattiker, A., Duvaud, S., Wilkins, M.R., Appel, R.D., and Bairoch, A., 2005, "Protein Identification and Analysis Tools on the ExPASy Server" in *The Proteomics Protocols Handbook*, Eds. Walker, J.M., Humana Press, NJ, US, 571–607.

[28] Kottarathil, A., Murugan, G., Rajkumar, D.S., Chandran, A.K., Elumalai, V., and Padmanaban, R., 2025, Designing multiepitope-based vaccine targeting immunogenic proteins of *Streptococcus mutans* using immunoinformatics to prevent caries, *The Microbe*, 7, 100320.

[29] Doytchinova, I.A., and Flower, D.R., 2007, VaxiJen: A server for prediction of protective antigens, tumour antigens and subunit vaccines, *BMC Bioinf.*, 8 (1), 4.

[30] Dimitrov, I., Bangov, I., Flower, D.R., and Doytchinova, I., 2014, AllerTOP v.2—A server for *in silico* prediction of allergens, *J. Mol. Model.*, 20 (6), 2278.

[31] Wei, L., Ye, X., Sakurai, T., Mu, Z., and Wei, L., 2022, ToxIBTL: Prediction of peptide toxicity based on information bottleneck and transfer learning, *Bioinformatics*, 38 (6), 1514–1524.

[32] Waterhouse, A., Bertoni, M., Bienert, S., Studer, G., Tauriello, G., Gumienny, R., Heer, F.T., de Beer, T.A.P., Rempfer, C., Bordoli, L., Lepore, R., and Schwede, T., 2018, SWISS-MODEL: Homology modelling of protein structures and complexes, *Nucleic Acids Res.*, 46 (W1), W296–W303.

[33] Singh, A., Copeland, M.M., Kundrotas, P.J., and Vakser, I.A., 2024, GRAMM web server for protein docking, *Methods Mol. Biol.*, 2714, 101–112.

[34] Jendele, L., Krivak, R., Skoda, P., Novotny, M., and Hoksza, D., 2019, PrankWeb: A web server for ligand binding site prediction and visualization, *Nucleic Acids Res.*, 47 (W1), W345–W349.

[35] Kuriata, A., Gierut, A.M., Oleniecki, T., Ciemny, M.P., Kolinski, A., Kurcinski, M., and Kmiecik, S., 2018, CABS-flex 2.0: A web server for fast simulations of flexibility of protein structures, *Nucleic Acids Res.*, 46 (W1), W338–W343.

[36] Singh, N., and Li, W., 2019, Recent advances in coarse-grained models for biomolecules and their applications, *Int. J. Mol. Sci.*, 20 (15), 3774.

[37] Grote, A., Hiller, K., Scheer, M., Münch, R., Nörtemann, B., Hempel, D.C., and Jahn, D., 2005, JCat: A novel tool to adapt codon usage of a target gene to its potential expression host, *Nucleic Acids Res.*, 33 (Suppl. 2), W526–W531.

[38] Rosano, G.L., Morales, E.S., and Ceccarelli, E.A., 2019, New tools for recombinant protein production in *Escherichia coli*: A 5-year update, *Protein Sci.*, 28 (8), 1412–1422.

[39] Samad, A., Ahammad, F., Nain, Z., Alam, R., Imon, R.R., Hasan, M., and Rahman, M.S., 2022, Designing a multiepitope vaccine against SARS-CoV-2: An immunoinformatics approach, *J. Biomol. Struct. Dyn.*, 40 (1), 14–30.

[40] Rachmat, J., 2010, Improved methods for production and characterisation of Jembrana disease virus proteins, *Dissertation*, Faculty of Health Science, Murdoch University, Perth, Australia.

[41] Wang, J., Alekseenko, A., Kozakov, D., and Miao Y., 2019, Improved modeling of peptide-protein binding through global docking and accelerated molecular dynamics simulations, *Front. Mol. Biosci.*, 6, 112.

[42] Jespersen, M., Peters, B., Nielsen, M., and Marcatili, P., 2017, BepiPred-2.0: Improving sequence-based B-cell epitope prediction using conformational epitopes, *Nucleic Acids Res.*, 45 (W1), W24–W29.

[43] Abidi, A., 2018, Validation tools for predicted linear B-epitopes: Surface accessibility, *Southeast Eur. J. Soft Comput.*, 7 (1), 49–53.

[44] Agarwal, V., Tiwari, A., and Varadwaj, P., 2022, Prediction of suitable T and B cell epitopes for eliciting immunogenic response against SARS-CoV-2 and its mutant, *Network Model. Anal. Health Inf. Bioinf.*, 11 (1), 1.

[45] Mollazadeh, S., Bakhshesh, M., Keyvanfar, H., and Nikbakht Brujeni, G., 2022, Identification of cytotoxic T lymphocyte (CTL) epitope and design of an immunogenic multi-epitope of bovine ephemeral fever virus (BEFV) glycoprotein G for vaccine development, *Res. Vet. Sci.*, 144, 18–26.

[46] Andreatta, M., Karosiene, E., Rasmussen, M., Stryhn, A., Buus, S., and Nielsen, M., 2015, Accurate pan-specific prediction of peptide-MHC class II binding affinity with improved binding core identification, *Immunogenetics*, 67 (11-12), 641–650.

[47] Díaz-Dinamarca, D.A., Salazar, M.L., Castillo, B.N., Manubens, A., Vasquez, A.E., Salazar, F., and Becker, M.I., 2022, Protein-based adjuvants for vaccines as immunomodulators of the innate and adaptive immune response: Current knowledge, challenges, and future opportunities, *Pharmaceutics*, 14 (8), 1671.

[48] Arai, T.Y., 2021, Design of helical linkers for fusion proteins and protein-based nanostructures, *Methods Enzymol.*, 647, 209–230.

[49] Khatrawi, E.M., Ali, S.L., Ali, S.Y., Abduldayeva, A., and Alhegaili, A.S., 2025, Designing a multi-epitope vaccine targeting UPF0721 of meningitis-causing *Salmonella enterica* serovar Typhimurium strain L-4126 by utilizing immuno-informatics and *in silico* approaches, *Mol. Syst. Des. Eng.*, 10 (7), 549–566.

[50] Barreto, A.S., de Franca, M.N.F., dos Reis, T.L.S., Silva, J.A.B.M., Dos Santos, P.L., de Oliveira, F.A., da Silva, A.M., Magalhaes, L.S., Secco, D.A., Andrade, M.A.F., Porto, L.C., Rosa, D.S., Cavalcante, R.C.M., Corrêa, C.B., Sidney, J., Sette, A., de Almeida, R.P., and Palatnik-de-Sousa, C.B., 2025, Design and development of highly conserved, HLA-promiscuous T cell multiepitope vaccines against human visceral leishmaniasis, *Front. Immunol.*, 16, 1540537.

[51] Ayyagari, V.S., Venkateswarulu, T.C., Karlapudi, A.P., and Srirama, K., 2022, Design of a multi-epitope-based vaccine targeting M-protein of SARS-CoV2: An immunoinformatics approach, *J. Biomol. Struct. Dyn.*, 40 (7), 2963–2977.

[52] Gharazi, H., Doosti, A., and Abdizadeh, R., 2025, Brucellosis novel multi-epitope vaccine design based on *in silico* analysis focusing on *Brucella abortus*, *BMC Immunol.*, 26 (1), 46.

[53] Pandey, R.K., Ojha, R., Aathmanathan, V.S., Krishnan, M., and Prajapati, V.K., 2018, Immunoinformatics approaches to design a novel multi-epitope subunit vaccine against HIV infection, *Vaccine*, 36 (17), 2262–2272.

[54] Grosvirt-Dramen, A., Urbach, Z.J., Hurst, P.J., Kwok, C.E., Patterson, J.P., Wang, F., and Hochbaum, A.I., 2025, Hierarchical assembly of conductive fibers from coiled-coil peptide building blocks, *ACS Nano*, 19 (10), 10162–10172.

[55] Sakuma, K., Kobayashi, N., Sugiki, T., Nagashima, T., Fujiwara, T., Suzuki, K., Kobayashi, N., Murata, T., Kosugi, T., Tatsumi-Koga, R., and Koga, N., 2024, Design of complicated all-α protein structures, *Nat. Struct. Mol. Biol.*, 31 (2), 275–282.

[56] Thu, T.T.M., Co, N.T., Tu, L.A., and Li, M.S, 2019, Aggregation rate of amyloid beta peptide is controlled by beta-content in monomeric state, *J. Chem. Phys.*, 150 (22), 225101.

[57] MacRaild, C.A., Seow, J., Das, S.C., and Norton, R.S., 2018, Disordered epitopes as peptide vaccines, *Pept. Sci.*, 110 (3), e24067.

[58] Kakakhel, S., Ahmad, A., Mahdi, W.A., Alshehri, S., Aiman, S., Begum, S., Shams, S., Kamal, M., Imran, M., Shakeel, F., and Khan, A., 2023, Annotation of potential vaccine targets and designing of mRNA-based multiepitope vaccine against lumpy skin disease virus via reverse vaccinology and agent-based modeling, *Bioengineering*, 10 (4), 430.

[59] Paul, S.K., Saddam, M., Rahaman, K.A., Choi, J.G., Lee, S.S., and Hasan, M., 2022, Molecular modeling, molecular dynamics simulation, and essential dynamics analysis of grancalcin: An upregulated biomarker in experimental autoimmune encephalomyelitis mice, *Heliyon*, 8 (10), e11232.

[60] Shabbir, M.A., Amin, A., Hasnain, A., Shakeel, A., and Gul, A., 2025, Immunoinformatics-driven design of a multiepitope vaccine against nipah virus: A promising approach for global health protection, *J. Genet. Eng. Biotechnol.*, 23 (2), 100482.

[61] Mahafujul Alam, S.S., Mir, S.A., Samanta, A., Nayak, B., Ali, S., and Hoque, M., 2025, Immunoinformatics-based designing of a multiepitope cancer vaccine targeting programmed cell death ligand 1, *Sci. Rep.*, 15 (1), 12420.

[62] Alnuqaydan, A.M., and Eisa, A.A., 2024, Targeting polyprotein to design potential multiepitope vaccine against Omsk hemorrhagic fever virus (OHFV) by evaluating allergenicity, antigenicity, and toxicity using immunoinformatic approaches, *Biology*, 13 (9), 738.

[63] Waidyasooriya, H.M., Hariyama, M., and Kasahara, K., 2017, An FPGA accelerator for molecular dynamics simulation using OpenCL, *Int. J. Networked Distrib. Comput.*, 5 (1), 52–61.

[64] Wankowicz, S.A., de Oliveira, S.H., Hogan, D.W., van den Bedem, H., and Fraser, J.S., 2022, Ligand binding remodels protein side-chain conformational heterogeneity, *eLife*, 11, e74114.

[65] Shahraki, P.K., Kiani, R., Siavash, M., and Bemani, P., 2025, Design of a multiepitope vaccine against *Staphylococcus aureus* lukotoxin ED using *in silico* approaches, *Sci. Rep.*, 15 (1), 14517.

[66] Zaytsev, K., Bogatyreva, N., and Fedorov, A., 2024, Link between individual codon frequencies and protein expression: Going beyond codon adaptation index, *Int. J. Mol. Sci.*, 25 (21), 11622.

[67] Redwan, E.M., 2006, The optimal gene sequence for optimal protein expression in *Escherichia coli*: Principle requirements, *Arab J. Biotechnol.*, 9 (3), 493–510.

[68] Yin, D., Bai, Q., Zhang, J., Xu, K., and Li, J., 2020, A novel recombinant multiepitope protein candidate for the diagnosis of brucellosis: A pilot study, *J. Microbiol. Methods*, 174, 105964.

[69] Rosalez-Mendoza, S., Rubio-Infante, N., Monreal-Escalante, E., Govea-Alonso, D.O., Garcia-Hernandez, A.L., Salazar-Gonzales, J.A., Gonzales-Ortega, O., Paz-Maldonado, L.M.T., and Moreno-Fierros, L., 2014, Chloroplast expression of an HIV envelope-derived multiepitope protein: Towards a multivalent plant-based vaccine, *Plant Cell, Tissue Organ Cult.*, 116 (1), 111–123.

[70] Khan, S., Rizwan, M., Zeb, A., Eldeen, M.A., Hassan, S., Ur Rehman, A., Eid, R.A., Zaki, M.S.A., Albadrani, G.M., Altyar, A.E., Nouh, N.A.T., Abdel-Daim, M.M., and Ullah, A., 2022, Identification of a potential vaccine against *Treponema pallidum* using subtractive proteomics and reverse-vaccinology approaches, *Vaccines*, 11 (1), 72.

[71] Nogimori, T., Suzuki, K., Masuta, Y., Washizaki, A., Yagoto, M., Ikeda, M., Katayama, Y., Kanda, H., Takada, M., Minami, S., Kobayashi, T., Takahama, S., Yoshioka, Y., and Yamamoto, T., 2023, Functional changes in cytotoxic CD8+ T-cell cross-reactivity against the SARS-CoV-2 Omicron variant after mRNA vaccination, *Front. Immunol.*, 13, 1081047.

[72] Bhat, P., Leggatt, G., Waterhouse, N., and Frazer, I.H., 2017, Interferon-γ derived from cytotoxic lymphocytes directly enhances their motility and cytotoxicity, *Cell Death Dis.*, 8 (6), e2836.